Mitra.[6] The largest discrepancy, and the only one outside the combined experimental uncertainty of the two sets of measurements, is for the A_1(TO) phonon. We found the A_1(TO) phonon to be at (267 ± 1) cm^{-1}, whereas Brafman and Mitra found the value to be (273 ± 3) cm^{-1}. These apparent frequency shifts could be due to the presence of unwanted impurities in our nominally pure samples, and this could also explain the as yet unidentified 208-cm^{-1} line.

We wish to thank Dr. Deiter Langer and Dr. Y. S. Park of Aerospace Research Laboratories, Wright Patterson Air Force Base, Ohio for helpful discussions as well as for providing the ZnS vapor-grown platelet crystals for this work. The advice and efforts of Dr. Miles V. Klein, in whose laboratory this work was performed is gratefully acknowledged.

*This work was supported in part by the Advanced Research Projects Agency under Contract No. HC 15-67-C-0221.

†Present address: Department of Physics, University of Dayton, Dayton, Ohio 45409.

‡Present address: Behlen Laboratory of Physics, University of Nebraska, Lincoln, Neb. 68508.

[1]A. R. Verma and P. Krishna, *Polymorphism and Polytypism in Crystals* (Wiley, New York, 1966).

[2]Lyle Patrick, Phys. Rev. 167, 809 (1968).

[3]D. W. Feldman, James H. Parker, Jr., W. J. Choyke, and Lyle Patrick, Phys. Rev. 173, 787 (1968), and references therein.

[4]H. Poulet, W. E. Klee, and J. P. Mathieu, in *Proceedings of the International Conference on Lattice Dynamics, Copenhagen*, 1963 (Pergamon, New York, 1965), pp. 337–341.

[5]W. G. Nilsen, Phys. Rev. 182, 838 (1969).

[6]O. Brafman and S. S. Mitra, Phys. Rev. 171, 931 (1968).

[7]J. F. Vetelino, S. S. Mitra, O. Brafman, and T. C. Damen, Solid State Commun. 7, 1809 (1969).

[8]Atsuko Ebina and Tadashi Takahashi, J. Appl. Phys. 38, 3079 (1967).

[9]G. V. Anan'eva, K. K. Dubenskii, A. I. Ryskin, and G. I. Khil'ko, Fiz. Tverd. Tela 10, 1800 (1968) [Sov. Phys. Solid State 10, 1417 (1968)].

[10]C. A. Arguello, D. L. Rousseau, and S. P. S. Porto, Phys. Rev. 181, 1351 (1969).

[11]T. C. Damen, S. P. S. Porto, and B. Tell, Phys. Rev. 142, 570 (1966).

[12]H. Jones, *The Theory of Brillouin Zones and Electronic States in Crystals* (North Holland, Amsterdam, 1960), Chap. 5.

[13]L. A. Feldkamp, G. Venkataraman, and J. S. King, Solid State Commun. 7, 1571 (1969); L. A. Feldkamp, D. K. Steinman, N. Vagelatos, J. S. King, and G. Venkataraman, J. Phys. Chem. Solids 32, 1572 (1971).

[14]S. P. S. Porto, J. A. Giordmaine, and T. C. Damen, Phys. Rev. 147, 608 (1966).

PHYSICAL REVIEW B VOLUME 6, NUMBER 4 15 AUGUST 1972

Optical Spectra of Some II-IV-V_2 Ternary Compounds

S. E. Stokowski*
Bell Telephone Laboratories, Murray Hill, New Jersey 07974
(Received 28 December 1972)

The polarized-reflectance spectra between 2.0 and 5.2 eV and the logarithmic derivative of the reflectance at 2 K for the ternary compounds $ZnSiAs_2$, $CdSiAs_2$, $CdSnAs_2$, and $CdSnP_2$ are reported. All the structure observed in previous electroreflectance data is seen in the logarithmic-derivative spectra plus some additional weak structure. The E_1 reflectance structures consist of three or more peaks; it is suggested that the additional splitting of the E_1 transitions is due to a separation in energy of the Λ and L critical points. No evidence is found in the optical spectra for the presence of Γ_{15}^v to X_1^c or X_3^c "pseudo-direct" transitions. The chalcopyrite crystalline structure, how it relates to zinc blende, its effect on the band structure, and group theory as applied to the chalcopyrites are discussed in detail.

I. INTRODUCTION

Interest in the I-III-VI_2 and II-IV-V_2 ternary compounds which crystallize in the chalcopyrite structure has been stimulated by their possible use as nonlinear optical materials[1,2] and as visible-emitting diodes. From a fundamental point of view a study of these compounds is a logical step in extending present knowledge about the properties of A^NB^{8-N} binary materials to the next-higher level of complexity; in these ternary compounds one is dealing with two different bonds rather than the single bond of the binaries. The optical spectra of the chalcopyrites is one very important property which can provide information about the band structure and thus, the bonding of these compounds. In particular, the experimentally obtained logarithmic derivative of the reflectance can provide a direct test for any band calculation. In this paper the optical spectra (reflectance and logarithmic

derivative of the reflectance) of the four II-IV-V_2 compounds $CdSiAs_2$, $ZnSiAs_2$, $CdSnAs_2$, and $CdSnP_2$ are presented and discussed.

A fair amount of optical data[3-7] on various II-IV-V_2's, mostly using the electroreflectance technique,[8-12] have appeared in the literature. However, the earlier direct-reflectance data have rather poor energy resolution, and therefore, could not provide a direct comparison with the sharp structure observed in electroreflectance. The present work is the first in which high-resolution reflectance data have been taken. All the structures seen in electroreflectance plus some additional weak transitions were observed.

This study is intended to provide a basis for future observations on the optical spectra of chalcopyrite compounds. The large amount of structure in the reflectance spectra and the absence of good band-structure calculations precludes the identification of most of the structure at this time. I have, though, grouped together the common features of the optical spectra for the four compounds, and discussed at length possible assignments of the E_1 structure. Further, no evidence is found for the presence of the "pseudo-direct" Γ_{15} to X_1 transition in the optical spectra. (The term "pseudo-direct" was introduced by Shay *et al.*[8] to describe a transition that was indirect in zinc blende, but which becomes direct in chalcopyrite because of the reduced Brillouin zone.)

In Sec. II is a detailed discussion of the chalcopyrite crystalline structure, how it relates to zinc blende, its effect on the band structure, and group theory as applied to the chalcopyrites. In Sec. IV the results are presented and discussed. In analyzing the optical spectra of the II-IV-V_2 materials I have taken the attitude that the major features in the spectra of the III-V compounds will appear in the chalcopyrites, but with additional splittings and structure due to the more-complex band structure. The availability of straight reflectance data helps in this regard since they are more easily compared to the III-V optical properties than the logarithmic derivative or electroreflectance data. Most of the discussion in Sec. IV concerns the E_1 reflectivity structures. It is suggested that the appearance of additional reflectance peaks in the E_1 region may be due to the energy separation of the Λ and L critical points.

II. CRYSTALLINE STRUCTURE AND GROUP THEORY

Most of the II-IV-V_2 compounds have the chalcopyrite structure (space group D_{2d}^{12} [$I\bar{4}2d$]). This structure is similar to that of zinc blende, the differences being a doubling of the unit cell along the c direction, a tetragonal compression, and a distortion of the tetrahedral environment of the ions. It contains two additional structural parameters, the c/a ratio and the displacement (x) of the anions from the $(\frac{1}{4}\frac{1}{4}\frac{1}{4})$ positions. It was found by Abrahams and Bernstein[13] that the group-IV ion in $ZnSiP_2$ and $CdSiP_2$ is surrounded by a relatively undistorted tetrahedron of anions. If this feature of the crystalline structure is present in the other II-IV-V_2 compounds, then x and c/a are related through $x=\frac{1}{2}-\frac{1}{4}(c^2/2a^2-1)^{1/2}$. Thus, the c/a ratio appears to depend on the amount of distortion from a regular tetrahedron around the group-II-ion site.

The chalcopyrite Brillouin zone has one-fourth the volume of the corresponding zinc-blende zone. (Diagrams of the chalcopyrite unit cell and Brillouin zone can be found in the literature; for example, in Ref. 8.) In Fig. 1 I have illustrated the relation between the zinc-blende and chalcopyrite Brillouin zones for the (100) and (110) planes. The zinc blende $X_{zb}(0, 0, 2\pi/a)$, $W_{zb}(0, 2\pi/a, \pi/a)$, and $W_{zb}(2\pi/a, 0, \pi/a)$ points become Γ points in chalcopyrite. The Γ_{zb} to $X_{zb}(0, 0, 2\pi/a)$ and Γ_{zb} to $X_{zb}(2\pi/a, 2\pi/a, 0)$ lines are bisected by the $T(0, 0, \pi/a)$ and $N(\pi/a, \pi/a, 0)$ points, respectively. The $L_{zb}(\pi/a, \pi/a, \pi/a)$ point is mapped onto N; $\Delta_{zb}(0, k, 0)$ for $k>\frac{5}{4}(\pi/a)$ becomes the B line; and $\Lambda_{zb}(k, k, k)$ lies in the Ω plane $\{110\}$. Character tables for D_{2d}^{12} can be found in a paper by Sandrock and Treusch,[14] although their notation differs somewhat from that commonly used. They also appear in a paper by Chaldyshev and Pokrovskii.[15] In Tables I and II are reproduced the character tables for Ω and N. The space-group operations of D_{2d}^{12} are E, S_{4z}, S_{4z}^{-1}, C_{2z}, $\{C_{2x}|\vec{\tau}\}$, $\{C_{2y}|\vec{\tau}\}$, $\{\sigma_{xy}|\vec{\tau}\}$, and

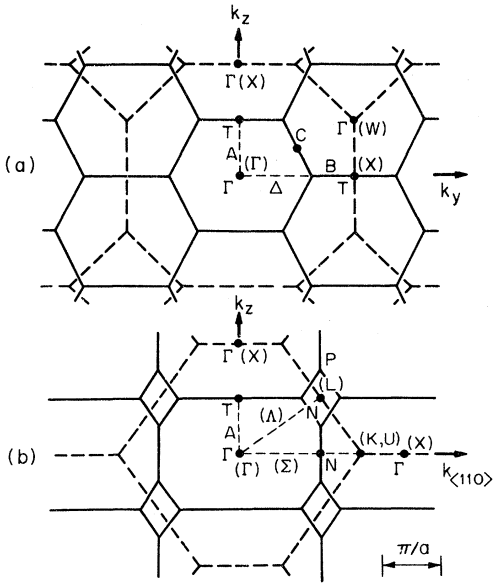

FIG. 1. Relation of the chalcopyrite (D_{2d}^{12}) Brillouin zone (solid line) to that of zinc blende (T_d^2) (dashed line) for the (100) and ($1\bar{1}0$) planes. The zinc-blende points and lines are labeled with parentheses.

TABLE I. Character table for the N point $(\pi/a, \pi/a, 0)$.

	$\{E\|0\}$	$\{\bar{E}\|0\}$	$\{C_{2z}\|0\}$	$\{\bar{C}_{2z}\|0\}$	$\{\sigma_{xy}\|\vec{\tau}\}$	$\{\bar{\sigma}_{xy}\|\vec{\tau}\}$	$\{\sigma_{x\bar{y}}\|\vec{\tau}\}$	$\{\bar{\sigma}_{x\bar{y}}\|\vec{\tau}\}$
N_1	2		0		0		0	
N_2	1	−1	i	$-i$	1	−1	i	$-i$
N_3	1	−1	i	$-i$	−1	1	$-i$	i
N_4	1	−1	$-i$	i	1	−1	$-i$	i
N_5	1	−1	$-i$	i	−1	1	i	$-i$

$\{\sigma_{x\bar{y}}|\vec{\tau}\}$ plus lattice translations, where $\vec{\tau} = (0, \frac{1}{2}a, \frac{1}{4}c)$. In Table III we show how some of the T_d^2 representations reduce to D_{2d}^{12} representations.

It is important to establish the differences between the chalcopyrite and zinc-blende structures since these affect the optical spectra. These differences are the following. (a) A compression along the c axis which transforms as the $3z^2 - r^2$ component of Γ_{12}. The magnitude of this compression is given by $1 - c/2a$ and varies from 0 for $ZnSnAs_2$ and $ZnSnP_2$ to 0.079 for $CdSiAs_2$. Values of $2 - c/a$ are given in Table IV. This tetragonal compression is equivalent to applying a uniaxial stress along $\langle 001 \rangle$ of a zinc-blende material. (b) A potential $V(X_4)$ due to an ordering of the group-II and group-IV ions which transforms as $X_4(0, 0, 2\pi/a)$ of T_d^2. Aong the c axis the group-II and group-IV ions alternate, whereas along the a axes they do not. There is no change in sign of this potential with interchange of the group-II and -IV ions, but it magnitude depends on the difference between the II-V and IV-V bonds. (c) An antisymmetric potential $V(W_1)$ which changes sign upon interchange of the group-II and -IV ions and transforms as $W_1(0, 2\pi/a, \pi/a) + W_1(2\pi/a, 0, \pi/a)$. The distortion of the zinc-blende tetrahedra is also included in this potential.

It would be useful if one could determine the magnitudes of these additional potentials in chalcopyrite from experimentally observed optical spectra. In order to do this, one must consider the effects of each one of the above potentials on the band structure of the chalcopyrites.

The tetragonal compression described in (a) can be considered a perturbation as in the framework of Hopfield's[16] quasicubic model. Its effect on the E_0 transitions has been discussed by Rowe and Shay,[17] and they find the quasicubic model fits the available experimental data quite well. Its magnitude for the E_0 transitions is of the order of 0.1 eV and is given by Δ_{cr} in Table IV.

The chalcopyrite potential which transforms as X_4 of T_d^2 allows an indirect Γ to X transition in zinc blende to become a direct transition in chalcopyrite. Its magnitude is of interest because many of the high-band-gap III-V materials have indirect gaps from Γ to X. In the corresponding chalcopyrites the transitions at these gaps would be direct, but their intensity depends on the magnitude of $V(X_4)$. The two indirect transitions of interest are Γ_{15}^v to X_1^c and Γ_{15}^v to X_3^c of T_d^2. The $X_1(0, 0, 2\pi/a)$ and $X_3(0, 0, 2\pi/a)$ points of T_d^2 become Γ_2 and Γ_3 in chalcopyrite (Table III). The Γ_{15}^v band splits into Γ_5^v and Γ_4^v in D_{2d}^{12}. The Γ_5^v to Γ_2^c and Γ_5^v to Γ_3^c transitions are allowed in σ polarization ($\vec{E} \perp \vec{c}$). There are no allowed transitions from Γ_4^v to Γ_2^c or Γ_3^c.

The "pseudo-direct" I_{15}^v to X_1^c or X_3^c transitions could be identified in chalcopyrite since they should appear primarily in σ polarization and consist of two structures with a splitting identical to that of the B and C components of the E_0 transitions. (This splitting arises from the spin-orbit split Γ_5^v state.) They should also fall a few tenths of an electron volt lower in energy than the E_2 transitions, using the III-V compounds as a guide. However, so far no optical structure which meets these conditions has been seen either in reflectance or electroreflectance spectra. Thus, as far as the Γ_{15}^v to X_1^c or X_3^c transitions are concerned, it would appear that the X_4 potential can be considered as a small perturbation on the zinc-blende structure.

The antisymmetric potential $V(W_1)$ will also give rise to "pseudo-direct" transitions between Γ and W, L and N, etc. of T_d. Knowledge of the strength

TABLE II. Character table for the Ω plane $(k_x = -k_y)$; $\lambda = e^{i[k_y(a/2)+k_z c]}$.

	$\{E\|0\}$	$\{\bar{E}\|0\}$	$\{\sigma_{x\bar{y}}\|\vec{\tau}\}$	$\{\bar{\sigma}_{x\bar{y}}\|\vec{\tau}\}$
Ω_1	1		λ	
Ω_2	1		$-\lambda$	
Ω_3	1	−1	$i\lambda$	$-i\lambda$
Ω_4	1	−1	$-i\lambda$	$i\lambda$

TABLE III. Compatibility tables for reduction of T_d^2 representations to D_{2d}^{12}.

	Representations			
	T_d^2	D_{2d}^{12}	T_d^2	D_{2d}^{12}
$\vec{k} = (0, 0, 0)$	Γ_1	Γ_1	Γ_6	Γ_6
	Γ_2	Γ_3	Γ_7	Γ_7
	Γ_3	$\Gamma_1 + \Gamma_3$	Γ_8	$\Gamma_6 + \Gamma_7$
	Γ_4	$\Gamma_2 + \Gamma_5$		
	Γ_5	$\Gamma_4 + \Gamma_5$		
$\vec{k} = (0, 0, 2\pi/a)$	X_1	Γ_2	X_6	Γ_6
	X_2	Γ_4	X_7	Γ_7
	X_3	Γ_3		
	X_4	Γ_1		
	X_5	Γ_5		
$[\vec{k} = (0, 2\pi/a, \pi/a)$	W_1	$\Gamma_1 + \Gamma_2$	$W_5 + W_6$	$2\Gamma_6$
$+\vec{k} = (2\pi/a, 0, \pi/a)]$	W_3	$\Gamma_3 + \Gamma_4$	$W_7 + W_8$	$2\Gamma_7$
	$W_2 + W_4$	$2\Gamma_5$		
$[\vec{k} = (\pi/a, \pi/a, \pi/a)$	L_1	N_1	L_4	$N_2 + N_5$
	L_2	N_1	L_5	$N_3 + N_4$
$\vec{k} = (\pi/a, \pi/a, -\pi/a)]$	L_3	$2N_1$	L_6	$N_2 + N_3 + N_4 + N_5$
$\vec{k} = (k, k, k)$	Λ_1	Ω_1	Λ_4	Ω_3
	Λ_2	Ω_2	Λ_5	Ω_4
	Λ_3	$\Omega_1 + \Omega_2$	Λ_6	$\Omega_3 + \Omega_4$

TABLE IV. Energies of observed E_1 structure along with c/a ratios and valence-band parameters for several II-IV-V_2 compounds.

	(1)				(2)	(3)	(4)	(5)	
	$E_1(1)$	$E_1(2)$	$E_1(3)$	$E_1(4)$	$2-c/a$	Δ_0(eV)	Δ_{cn}(eV)	Δ_1(est.)	Ref.
$ZnSnAs_2$	2.26	2.32	2.55		0	0.34	0	0.23	11
$ZnGeAs_2$	2.26	2.41	2.74	2.92	0.034			0.2	11
$ZnSiAs_2$	2.74	2.90	3.25		0.057	0.28	−0.15	0.19	9,11
	2.84	2.99	3.09	{3.23 3.34}					a
$CdSnAs_2$	2.13	2.23	2.43	2.62	0.044	0.5	0.03	0.33	11,b
	2.13	2.23	2.50	2.70					a
$CdGeAs_2$	2.18	2.32	2.49	2.65	0.112			0.25	11
	{2.02 2.09}	2.29	2.44	2.60					10
$CdSiAs_2$	2.50	2.57	2.99	3.10	0.151	0.29	−0.39	0.23	10
	2.62	{2.69 2.72}	3.09	3.20					a
$CdSnP_2$	2.56	2.69	2.90	3.00	0.048	0.10	−0.12	0.08	8
	2.68	2.77	2.99	3.07					a
$CdGeP_2$					0.123	0.11	−0.27	0.11	c

[a]This work.
[b]R. K. Karymshakov, Y. I. Ukhanov, and Y. V. Shmartsev, Fiz. Tekhn. Poluprov. 5, 514 (1971) [Sov. Phys. Semicond. 5, 450 (1971)].
[c]J. L. Shay, E. Buehler, and J. H. Wernick, Phys. Rev. B 4, 2479 (1971).

of such transitions relative to those which are direct in zinc blende would indicate whether one can consider $V(W_1)$ as a perturbation on the zinc-blende potential. If the so-called "pseudo-direct" transitions are relatively strong, then a perturbation treatment is not valid, in which case, it might be better to drop the term "pseudo-direct."

III. EXPERIMENTAL TECHNIQUES

The reflectance measurements were made with a sensitive double-beam spectrophotometer previously described.[18] The logarithmic derivative of the reflectance was obtained by numerical differentiation of the reflectance data using a digital computer. The signal-to-noise ratio was limited by shot noise in the case of $CdSnP_2$; however, for the other materials the largest noise source was variation of the reflected light due to sample vibration. This noise source becomes important when the reflecting surface is not smooth and flat. For $CdSnP_2$ the noise in the logarithmic derivative of the reflectance at 3.8 eV was 0.02 eV^{-1} with a resolution of 1.6 Å. The observed noise level in the data from the other materials was 0.05 eV^{-1} for $ZnSiAs_2$ and $CdSnAs_2$, and 0.03 eV^{-1} for $CdSiAs_2$.

The $CdSiAs_2$ and $ZnSiAs_2$ crystals were grown by Buehler and Wernick by a chemical-transport technique described previously[9]; the $CdSnP_2$ and $CdSnAs_2$ were grown from a tin solution, as described in Ref. 19. The materials are of unknown purity. The crystallographic planes from which the reflectance was obtained are {112} planes. The surface preparation was as follows: $ZnSiAs_2$—"Syton" polished; $CdSiAs_2$— etched 1 min in methanol–1%-bromine solution; $CdSnP_2$—as-grown surface; and $CdSnAs_2$—as-grown surface. In $CdSiAs_2$ and $ZnSiAs_2$ the surface treatment did sharpen the structure a bit and increased the uv reflectance by a few percent, but otherwise had no effect. A word of caution here; too much significance to weak structure must not be assigned since it may not be reproduced when higher-purity samples or better surface treatments are available.

IV. RESULTS

A. General Features

The polarized reflectances and $(1/R)dR/dE$ at 2 K for the four substances studied here are shown in Figs. 2 and 3, respectively. Only two-thirds of the intensity in the $\vec{E} \parallel [111]$ polarized spectra comes from the $\vec{E} \parallel [001]$ spectra since the reflecting plane is {112}. I have not made any attempt to obtain absolute values for the reflectance because of the poor quality of the sample surfaces. The reflectance values given in Fig. 2 are from the uncorrected raw data. However, the observed reflectance differs from the true reflectance by a scaling factor which varies very slowly with energy, if at all. The logarithmic derivative values, which do not contain this scaling factor, are to be taken as absolute.

The reflectance features are about 0.1 eV lower

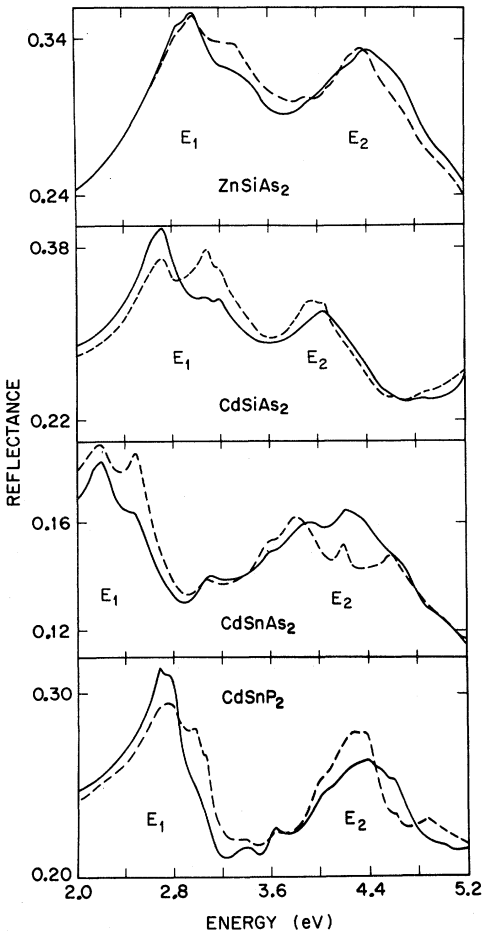

FIG. 2. Polarized reflectance spectra at 2 K. The spectra for light polarized $\vec{E} \perp [001]$ are given by the dashed line; for light polarized $\vec{E} \parallel [111]$, by the solid line. The reflecting planes are $(11\bar{2})$.

in energy at 300 K. My data are consistent with those obtained by Shay *et al.*[8-10] at 300 K by electroreflectance techniques. A comparison of our data at 300 K and that of Shay *et al.* shows that the reflectance and electroreflectance structures are within 0.02 eV of each other. There are some differences between their data and mine as to the relative intensities of the peaks in the two polarizations. I also observe more structure at 2 K than that seen in reflectance and electroreflectance at 300 K.

The first feature to note is the appearance of three or more structures in the E_1 region, in contrast to the zinc-blende materials for which only two peaks (E_1 and $E_1+\Delta_1$) are seen. This additional splitting of the E_1 peaks has been observed in all chalcopyrite materials so far. Higher in energy there is an abundance of structure. There are, however, between 4.0 and 4.5 eV, peaks which appear to be associated with the E_2 structure of zinc-blende materials. It is interesting that the E_2 region has a lower reflectivity value than the E_1 region. This is in contrast to the III-V materials, where the E_2 peak has a higher reflectance than E_1. This ratio could partially be explained by the larger increase in the E_2 width in going from zinc blende to chalcopyrite. In Table V are listed all the observed reflectance structures in common groupings according to their energies and polarizations.

The larger number of reflectance structures in the chalcopyrites as compared to zinc-blende substances can arise from the lifting of degeneracies in zinc blende, which are of two types. These two types are: degeneracies within the representations of the group of the k vector (band degeneracies) and the degeneracy of k vectors within a star of k (degeneracy of critical points). [For instance, the star of the X point of T_d^2 is split into two in chalcopyrite: $X_{zb}(2\pi/a, 0, 0)$ and $X_{zb}(0, 2\pi/a, 0)$ going to $T(0, 0, \pi/a)$, and $X(0, 0, 2\pi/a)$ to Γ.] Additional structure may also result from indirect transitions in zinc blende which become allowed in chalcopy-

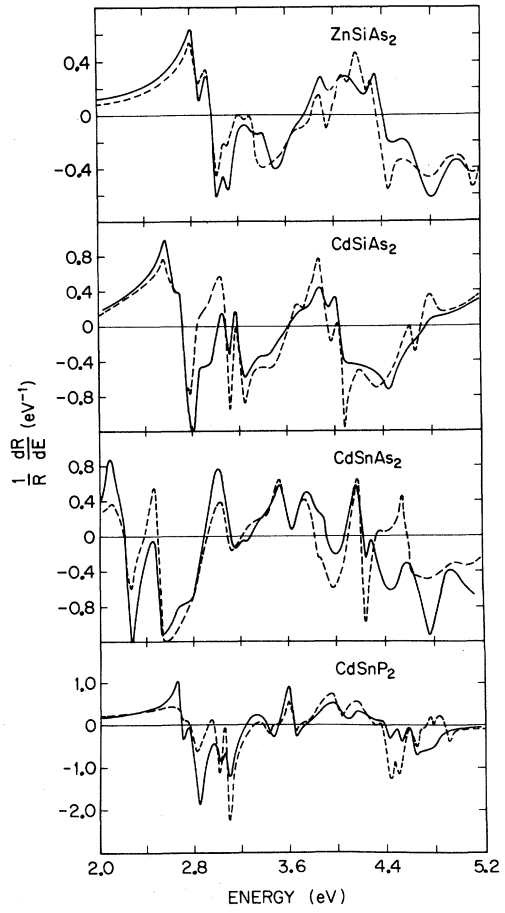

FIG. 3. Logarithmic derivative of the polarized reflectivity at 2 K. Light polarized $\vec{E} \perp [001]$—dashed line; $\vec{E} \parallel [111]$—solid line.

TABLE V. Energies of structures in the reflectance of four chalcopyrite materials at 2 K.[a]

		$ZnSiAs_2$	$CdSiAs_2$	$CdSnAs_2$	$CdSnP_2$
E_1	(1)	2.84 ∥ (⊥)	2.62 ∥ (⊥)	2.13 ∥ (⊥)	2.68 ∥(⊥)
	(2)	2.99	2.69 ⊥ (∥) 2.72 ∥ (⊥)	2.23	2.77
	(3)	3.09 ∥(⊥)	3.09 ⊥(∥)	2.50 ⊥(∥)	2.99 ⊥ (∥)
	(4)	3.23 ⊥, *w* 3.34 ⊥	3.20 ⊥(∥)	2.70	3.07 ⊥ (∥)
E_{c1}		3.45 ∥		3.08 ∥(⊥)	3.40 ∥ (⊥)
E_{c2}					3.62 ∥ (⊥)
E_{c3}	(1)	3.92 ⊥ (∥)	3.72 ⊥, *w*	3.58 ⊥(∥)	4.00 ⊥ (∥)
	(2)	4.09 ⊥ (∥)			4.06 ∥
E_2	(1)	4.23 ⊥ (∥)	3.92 ⊥(∥)	3.81 ⊥(∥)	4.28 ⊥ (∥)
	(2)	4.38 ⊥ (∥)	4.06 ⊥(∥)	3.90 ∥ (⊥)	4.40 ⊥ (∥)
	(3)	4.42 ∥	4.25 *w*	4.21 ⊥(∥)	4.48 ∥
	(4)	4.70 ∥ (⊥)	4.35 *w*	4.37 ∥	4.62 ∥ (⊥)
E_{c4}	(1)	4.90	4.65 ⊥	4.59 ⊥(∥)	4.88 ⊥
	(2)		4.85	4.68 ∥	
Weak structure		3.72	3.40	5.03	

[a] ∥ (⊥) signifies that the structure is stronger in $\vec{E}$ ∥ [111] polarized light, but does appear in $\vec{E}$ ⊥ [001]; similarly, for ⊥ (∥). The letter *w* indicates the structure is weak.

rite due to the reduced Brillouin zone. These were labeled "pseudo-direct" transitions by Shay *et al.*[8] The magnitude of these "pseudo-direct" transitions depends directly on the size of the potentials $V(X_4)$ and $V(W_1)$ as discussed in Sec. II. As also discussed there, the $V(X_4)$ potential does not seem to be large enough to give rise to observable reflectance structure resulting from the Γ_{15}^v to X_1^c "pseudo-direct" transitions. One could suggest, therefore, that other transitions allowed by $V(X_4)$ are weak in the absence of accidental degeneracies.

Certainly, lifting the zinc-blende degeneracies will increase the number of transitions considerably, and the majority of the observed structure in the chalcopyrites probably arises from this source. At this time, though, a definite statement cannot be made concerning the intensity of "pseudo-direct" transitions resulting from the chalcopyrite $V(W_1)$ potential. However, the appearance of reflectance peaks, labeled E_{c1} and E_{c2}, in the region of 3.1 to 3.6 eV, in which there is no structure present for III-V zinc-blende materials, does suggest that I may be seeing "pseudo-direct" transitions. If this were the case, their intensity indicates a sizable $V(W_1)$ potential. Definite identification, though, will have to await further experimental results and pseudopotential-band calculations.

B. E_1 Transitions

In the remainder of this section I discuss exclusively the reflectance structure in the E_1 region. (Assignments of the higher-energy reflectance peaks at this time would be premature since so little is known about the band structures.) The E_1 and $E_1+\Delta_1$ peaks in zinc-blende materials arise from Λ_3^v to Λ_1^c transitions along the ⟨111⟩ directions. Experimental evidence[20] indicates that a region of the Brillouin zone from the L point to about $(\pi/a) \times (0.2, 0.2, 0.2)$ contributes to the E_1 reflectance peaks. The Δ_1 splitting is simply the spin-orbit splitting of Λ_3^v. In most of the III-V compounds, we have $\Delta_1 \simeq \frac{2}{3}\Delta_0$, the so-called "two-thirds rule." If a compression is applied to the [001] axis, the splitting between the two E_1 peaks increases to

$$[(\Delta_1)^2 + \tfrac{1}{3}(\Delta_{cr})^2]^{1/2}, \tag{1}$$

where Δ_{cr} is a product of the tetragonal strain and the deformation potential b for the E_1 transitions. Also upon [001] compression the lower energy E_1 transition becomes stronger in π ($\vec{E} \parallel \vec{P}$); and $E_1 + \Delta_1$, stronger in σ ($\vec{E} \perp \vec{P}$).

One should be able to show how the E_1 structure in the chalcopyrites is derived from that of zinc-blende materials. The effect of the simple tetragonal compression can be determined quite easily. If one assumes the "two-thirds rule" to be applicable and Δ_{cr} to be k independent, then using the experimentally known values for Δ_0 and Δ_{cr}, one can estimate Δ_1 as indicated in column (5) of Table IV using Eq. (1). (For those materials in which Δ_0 and Δ_{cr} have not been determined, I use Δ_1 of the corresponding III-V compound.) These calculated values for Δ_1 are only rough estimates, considering the assumptions made in the calculation. Comparing the splittings of the E_1 structures listed in Table IV with the expected Δ_1, I find that there is reasonably good agreement except for $CdSiAs_2$, the material with the largest tetragonal compression. [For $CdSnP_2$ Δ_1 is estimated to be 0.08 eV; $E_1(1)$ and $E_1(2)$ are separated by 0.09 eV; $E_1(1)$ and $E_1(2)$ of $ZnSiAs_2$ are separated by 0.15 eV; the Δ_1(est) is 0.19 eV; and so on.]

As expected from the simple calculation the $E_1(1)$ structure is mainly π polarized in those materials for which polarized spectra are available. The other spin-orbit-split component, which should be σ polarized, is σ polarized for $CdSnAs_2$, but has no definite polarization in $CdSnP_2$, $ZnSiAs_2$, and $CdGeAs_2$.

I now come to the more interesting question of the origin for the additional structure in the E_1 region. The striking features of the spectra are that the $E_1(1) - E_1(2)$ and $E_1(3) - E_1(4)$ energy differences are approximately equal and that the $E_1(3)$ and $E_1(4)$ peaks are strongly σ polarized except in $ZnSiAs_2$. It is apparent that there is an additional perturbation besides spin-orbit coupling which can split the E_1 transitions. In order to discuss possible sources of this perturbation we must first go back to discuss the group theory and selection rules for the E_1's.

As can be seen in Fig. 1, the Λ line is separated

into two pieces in chalcopyrite, the zone boundary occurring at $\frac{5}{6}(\pi/a)(1,1,1)$. The Λ line lies in the Ω plane (character table—Table II) and L maps into the N point (character table—Table I). Due to the $V(X_4)$ and $V(W_1)$ chalcopyrite potentials, the Λ bands can interact with bands on lines from X to L and from W to N. Let us consider each of the two segments of the Λ line separately, starting with the Λ line for $k<\frac{5}{6}(\pi/a)(1,1,1)$. In the absence of spin-orbit coupling, the Λ_3^v band of T_d^2 splits into the Ω_1^v and Ω_2^v bands of D_{2d}^{12}; the Λ_1^c band becomes the Ω_1^c band. The Ω_1^v to Ω_1^c transition is polarized in both σ and π; the Ω_2^v to Ω_1^c, only in σ. Upon the addition of spin-orbit coupling Ω_1 and Ω_2 both split into $\Omega_3+\Omega_4$. Thus, the former Λ_3^v band consists of two $\Omega_3+\Omega_4$ pairs; and the Λ_1^c band, of one $\Omega_3+\Omega_4$ pair. Because of the absence of inversion symmetry the $\Omega_3+\Omega_4$ pair is not required to be degenerate. However, in zinc blende the equivalent splitting (of Λ_4^v and Λ_5^v), which is related to the linear-k term in the Γ_8^v band, is of order 10^{-5} eV. One should also expect the $\Omega_3-\Omega_4$ splitting in chalcopyrite to be quite small because of time-reversal symmetry. Thus, I conclude that this part of the Λ line should give rise to two reflectivity structures, one mainly σ polarized, the other π polarized.

The band structure around the L point is considerably more complicated. With or without spin-orbit coupling all bands are doubly degenerate at N (N_2, N_4 and N_3, N_5 are degenerate because of time-reversal symmetry). The part of the Λ bands from $\frac{5}{6}(\pi/a)(1,1,1)$ to L are joined by bands along the $X(0,0,-2\pi/a)$ to $L(\pi/a,\pi/a,-\pi/a)$ line of zinc blende. However, since these two L points are mapped onto $N(\pi/a,-\pi/a,0)$, there are bands from the region around the $(\pi/a,-\pi/a,0)$ point of T_d^2 present here also. Of particular importance is the observation that the Λ_3^v band at L is approximately degenerate with the Σ_1^v band at $(\pi/a,\pi/a,0)$ in the zinc-blende materials. This means that there are three N_1^v bands with relatively closely spaced energies in the chalcopyrites. This can be seen in the calculations of Poplavnoi *et al.*[21] The interaction between the Σ_1^v band at $(\pi/a,\pi/a,0)$ and the L_3^v band, which comes about because of the antisymmetric potential $V(W_1)$ very likely shifts the energies of the L_3^v to L_1^c transitions relative to the Λ_3^v to Λ_1^c transitions. I propose that this is the probable source of the additional splitting. The interaction between L_3^v and Σ_1^v will also allow some intensity for the "pseudo-direct" Σ_1^v to L_1^c transition; therefore, additional structure may be present which is due to these "pseudo-direct" transitions.

There have been other suggestions as to the origin of the E_1 structure. Shay *et al.*[8] assigned the $E_1(3)$ and $E_1(4)$ of $CdSnP_2$ peaks to "pseudo-direct" transitions from the Σ line to the $L-W$ line and to a "pseudo-direct" X to Γ transition. The four E_1 transitions of $CdSnP_2$ were assigned to the N point by Kavaliauskas *et al.*[12] They suggested that the 0.08-eV separation between $E_1(1)$, $E_1(3)$ and $E_1(2)$, $E_1(4)$ arises from the splitting between $N_2^v+N_4^v$ and $N_3^v+N_5^v$. I argued above that this splitting is likely to be small. For $ZnSiAs_2$, Kwan and Woolley[11] assigned $E_1(2)$ and $E_1(4)$ to E_1 and $E_1+\Delta_1$ on the argument that the 0.14-eV separation between $E_1(1)$ and $E_1(2)$ was too small to be Δ_1.

Once definite identification of the E_1 structures can be made, one may be able to say something about the magnitude of the antisymmetric potential $V(W_1)$, which could provide a useful comparison with theoretical calculations. To help in the identification more materials should be studied, in particular, the phosphides, which have a much smaller spin-orbit splitting. A much better estimate of Δ_1 than that provided by Eq. (1) is needed to provide us with that important parameter. At this time it is perhaps best to await a pseudopotential calculation of $(1/R)dR/dE$ to check this hypothesis of an energy separation between the Λ and L critical points.

ACKNOWLEDGMENTS

I wish to acknowledge helpful discussions with J. E. Rowe, D. D. Sell, and J. L. Shay. I particularly thank E. Buehler and J. Wernick for the loan of the samples.

---

*Present address: Research Institute for Advanced Studies, 1450 South Rolling Road, Baltimore, Md. 21227.

[1]G. D. Boyd, W. B. Gandrud, and E. Buehler, Appl. Phys. Letters 18, 446 (1971).

[2]R. L. Byer, H. Kildal, and R. S. Feigelson, Appl. Phys. Letters 19, 237 (1971).

[3]$CdSnAs_2$: G. A. Sikharulidze, V. M. Tuchkevich, Y. I. Ukhanov, and Y. V. Shmartsev, Fiz. Tekhn. Poluprov. 1, 309 (1967) [Sov. Phys. Semicond. 1, 254 (1967)]; L. B. Zlatkin and E. K. Ivanov, *ibid.* 3, 926 (1969) [3, 781 (1969)].

[4]$ZnSiP_2$ and $ZnSiAs_2$: F. P. Kesamanly, S. G. Kroitoru, Y. V. Rud', V. V. Sobolev, and N. N. Syrbu, Dokl. Akad. Nauk SSSR 163, 868 (1965) [Sov. Phys. Doklady 10, 743 (1966)].

[5]$ZnSiP_2$: I. K. Akopyan and L. B. Zlatkin, Dokl. Akad. Nauk SSSR 168, 547 (1966) [Sov. Phys. Doklady 11, 435 (1966)].

[6]$ZnSnP_2$: N. A. Goryunova, M. L. Belle, L. B. Zlatkin, G. V. Loshakova, A. S. Poplavnoi, and V. A. Chaldyshev, Fiz. Tekhn. Poluprov. 2, 1344 (1968) [Sov. Phys. Semicond. 2, 1126 (1969)].

[7]V. V. Sobolev and V. I. Donetskikh, Fiz. Tverd. Tela 12, 2716 (1970) [Sov. Phys. Solid State 12, 2183 (1971)].

[8]J. L. Shay, E. Buehler, and J. H. Wernick, Phys. Rev. B 2, 4104 (1970).

[9]J. L. Shay, E. Buehler, and J. H. Wernick, Phys. Rev. B 3, 2004 (1971).
[10]J. L. Shay and E. Buehler, Phys. Rev. B 3, 2598 (1971).
[11]C. C. Y. Kwan and J. C. Woolley, Can. J. Phys. 48, 2085 (1970); Phys. Status Solidi 44, K93 (1971); Appl. Phys. Letters 18, 520 (1971).
[12]J. Kavaliauskas, G. F. Karavaev, E. I. Leonov, V. M. Orlov, V. A. Chaldyshev, and A. Sileika, Phys. Status Solidi 45, 443 (1971).
[13]S. C. Abrahams and J. L. Bernstein, J. Chem. Phys. 55, 796 (1971).
[14]Von R. Sandrock and J. Treusch, Z. Naturforsch. 19a, 844 (1964).
[15]V. A. Chaldyshev and V. N. Pokrovskii, Izv. Vysshikh Uchebn. Zavedenii Fiz. 2, 173 (1960).
[16]J. J. Hopfield, J. Phys. Chem. Solids 15, 97 (1960).
[17]J. E. Rowe and J. L. Shay, Phys. Rev. B 3, 451 (1971).
[18]D. D. Sell, Appl. Opt. 9, 1926 (1970).
[19]E. Buehler, J. H. Wernick, and J. L. Shay, Mater. Res. Bull. 6, 303 (1971).
[20]S. Koeppen, P. Handler, and S. Jasperson, Phys. Rev. Letters 27, 265 (1971).
[21]A. S. Poplavnoi, Yu. I. Polpavnoi, and V. A. Chaldyshev, Izv. Vysshikn Uchebn. Zavedenii Fiz. 7, 17 (1970); 6, 95 (1970).

PHYSICAL REVIEW B VOLUME 6, NUMBER 4 15 AUGUST 1972

Electroreflectance and Band Structure of $Ga_xIn_{1-x}P$ Alloys

C. Alibert and G. Bordure
Centre d'Etude d'Electronique du Solide, 34 Montpellier, France

and

A. Laugier and J. Chevallier
Laboratoire de Physique des Solides, Centre National de la Recherche Scientifique, 92 Meudon, Bellevue, France

(Received 24 March 1972)

The electroreflectance spectra of solution-grown $Ga_xIn_{1-x}P$ alloys were measured at room temperature in the whole range of composition. The variation of the E_0, E_1, E_0', and E_2 energies with concentration is reported: It is parabolic for E_0 and E_1, and approximately linear for E_0' and E_2. Except for E_1 these results agree with the calculation of the band structure by the dielectric two-band method in the virtual-crystal approximation including the effect of disorder. The latter effect is found small. For E_1 the deviation from a linear variation is larger than calculated. E_1 exhibits another interesting anomaly: Its spin-orbit splitting is maximum for $x = 0.5$. The $\vec{k} \cdot \vec{p}$ method is used to calculate some band parameters from our data. The $\Gamma - X$ conduction-band crossover energy E_c and composition x_c are accurately determined using the E_0 vs x curve and the indirect gaps obtained from optical absorption: $x_c = 0.63 \pm 0.015$, $E_c = 2.14 \pm 0.01$ eV.

I. INTRODUCTION

The $Ga_xIn_{1-x}P$ semiconducting alloys form a continuous, single-phase, solid solution throughout the whole composition range. They have received increased attention recently because of the large direct band gap attainable. In these ternary alloys, direct transitions are possible with photon energies up to 2.15 eV, which makes it a potentially efficient electroluminescent source of light in the range of highest sensitivity of the human eye.[1-3]

The energy-band structures of GaP and InP have been calculated theoretically[4,5] and a large number of experimental results have yielded band-structure parameters. However, the band structure of $Ga_xIn_{1-x}P$ is not so well known. There has been disagreement about the value of the "crossover" composition x_c at which the energy of the Γ and X conduction-band minima becomes equal. From measurements on diodes, Lorenz *et al.*[2] determined $x_c = 0.8$. Measurements of the band-edge absorption coefficient as a function of photon energy by Rodot *et al.*[3] determined $x_c = 0.63$. This value has been confirmed by Williams *et al.*[6] and White *et al.*[7] using photoluminescence-excitation spectra, by Hakki *et al.*[8] using hydrostatic-pressure experiments and by photoluminescence at low temperature.[9] However, assigning the cathodo luminescence peaks at 300 °K to the band gap, some authors[10,11] give $x_c = 0.74$ with a parabolic-empirical variation of the direct band gap, $E_d = 1.34 + 1.426x + 0.758x(x-1)$. Onton and Chicotka[12] estimate that their low-temperature-photo-